ELSEVIER

Journal of Molecular Catalysis A: Chemical 141 (1999) 39–55

JOURNAL OF MOLECULAR CATALYSIS A: CHEMICAL

Atomic-scale mechanism for the activation of catalyst surfaces

Ken-ichi Tanaka *, Naoki Takehiro

The Institute for Solid State Physics, The University of Tokyo, 7-22-1 Roppongi, Minato-ku, Tokyo 106, Japan

Abstract

The hydrogenation and the isomerization of olefins on MoS_2 proceed via alkyl intermediates but are independent catalysis, which is inconsonant to the Horiuti–Polyani mechanism for the isomerization and hydrogenation reactions. Detailed studies proved that the hydrogenation reaction proceeds on di-hydride (MoH_2) sites and the isomerization reaction takes place on mono-hydride (MoH) sites although both sites are formed on the edge surface of MoS_2 in the presence H_2. More dramatic chemical activation was shown with an inactive MoO_x surface, where the formation of Mo-alkylidene sites the changes MoO_x inert surface a super-active olefin metathesis catalyst. Chemical activation is also recognised on well defined surfaces. Catalytic reaction of $NO + H_2 \rightarrow 1/2\ N_2 + H_2O$ is highly structure sensitive on Pt(100), Pt(110), Rh(100), and Rh(110) surfaces while the reaction is entirely structure insensitive on such bimetallic surfaces as Pt/Rh(100), Rh/Pt(100), Pt/Rh(110), and Rh/Pt(110). It was deduced that formation of active sites having a common local structure is responsible for the structure sensitive catalysis. Complexity of the activation process of bimetallic surface is shown in atomic-scale on a Cu/Pd(111) surface by STM. Base on these results, we could conclude that the optimized catalysts are structure insensitive because their surface will preserve the highest density sites.

Keywords: Active sites; Hydrogenation and isomerization of olefins; Olefin metathesis reaction; NO reduction; Reconstructive activation; Pt on Rh and Rh on Pt single crystal bimetallic catalysts; Cu/Pd(111); STM; MoS_2; MoO_x

1. Introduction

A catalytic reaction is composed of a series of elementary reactions and the kinetic feature of the reaction depends on the slowest step(s) among them. Based on this concept, Horiuti [1] pointed out the importance of the stoichiometric number of the rate determining elementary reaction. This concept suggests us that the surface during catalysis depend on the rate determining step(s), and as Tamaru [2,3] pointed out, the rate determining slow step could be deduced by measuring the adsorption during catalysis. From this view point, he was very much interested in the direct measurements of the catalyst surface during the course of reaction, and he developed the in-situ adsorption measurement method and applied the in-situ spectroscopy to deduce the dynamical behaviour of the adsorbed species.

* Corresponding author. Tel.: +81-3-3478-7811; Fax: +81-3-3401-5169

1381-1169/99/$ - see front matter
PII: S1381-1169(98)00248-9

On the other hand, it has been a long standing puzzle that why we can bear only empirical procedures for getting optimum industrial catalysts. To this question, Boudart et al. [4] pointed out an interesting feature of the heterogeneous catalysis, that is, the catalytic reactions can be classified into the two types, one is facile reaction but the other is demanding reaction. Bernasek et al. [5] substantiated this interesting feature on well defined single crystal surfaces as a phenomenon of the structure sensitive and structure insensitive catalysis.

In the last 10 years, a new exploration in the atomic scale studies throw a new light on the activation mechanism of the catalyst on well defined surfaces. One dramatic result is the ammonia synthesis reaction on single crystal Fe surfaces given by Somorjai et al. [6,7]. Ammonia synthesis reaction on Fe single crystal strongly depends on the crystallographic surface structures, that is, Fe(111) ≫ Fe(100) > Fe(110). However, the catalytic activity of the Fe(100) and Fe(110) surfaces are dramatically improved when the surfaces are covered with a $FeAl_2O_4$ over-layer. By the TPD experiments, they deduced that a Fe(111) like over-layer is grown on the $FeAl_2O_4$ over-layer when the surface is heated in a mixture of $N_2 + H_2$ at 673 K. As a result, the Fe(100) and Fe(110) surfaces have almost equal activity at Fe(111) surface, that is, the Fe surface changes to structure insensitive catalyst by adding alumina.

Another interesting activation was found on a Pt–Rh(100) alloy and Rh/Pt bimetallic surfaces by Tanaka et al. [8–11], where an active surface having a common local structure is constructed on the Pt–Rh(100) alloy as well as on the bimetallic surfaces [12,13]. Our understanding of the surface is markedly progressed in the last 10 years, and it would be possible to gain an insight of the activation mechanism of the catalysts so far it has been borne by empirical ways. It is note worthy fact that the reaction intermediates should be considered in relation to the elementary steps when we discuss the active sites [14].

2. Formation of active sites during catalysis

Isomerization reaction of olefins via alkyl intermediates have been explained for long time in relation to the hydrogenation reaction by a mechanism of so called Horiuti–Polanyi mechanism [15,16]. As described in Eq. (1), it was tacitly assumed that the alkyl species are common intermediates for the hydrogenation and isomerization reactions as well as for the hydrogen exchange of olefins. If this mechanism would be the case, intermediates of the hydrogenation of olefins could be deduced by the isotopic exchange reaction of olefins.

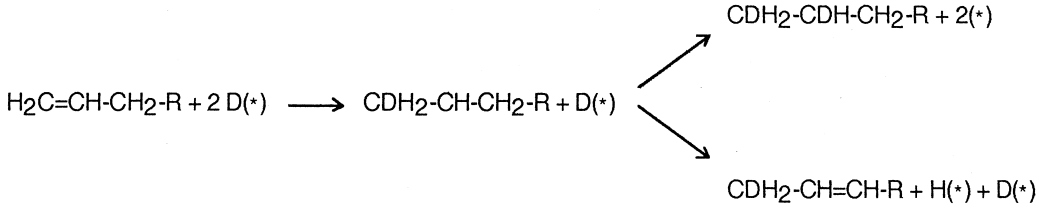

(1)

Unfortunately, the real catalysis is not the case as has been clearly shown by Tanaka [14]. And now, we can state that ‘any catalytic reactions should involve at least one unique elementary reaction or process by which each catalytic reaction can be distinguished’. The hydrogenation and the isomerization reactions of olefin via alkyl intermediates are a good example. It is obvious that the hydrogenation of alkyl intermediates is a necessary elementary reaction for the hydrogenation reaction

but is not the required process for the isomerization reaction of olefins. It is also truth that an internal rotation of alkyl intermediates is a necessary process for the isomerization reaction but is not required for the hydrogenation reaction.

Isomerization reaction of *n*-butenes and their hydrogenation reaction are concomitantly promoted on MoS_2 crystal surface by adding hydrogen, which reveals that these two reactions may proceed via alkyl intermediates. When D_2 was added to but-1-ene, however, it was found that the hydrogenation reaction yielded butane-1,2-d_2 in more than 80% but the but-2-ene produced by the isomerization reaction was but-2-ene-d_0 in almost 100%. This fact indicates that the intermediate for the isomerization reaction is *sec*-butyl-d_0 in nearly 100% while the hydrogenation reaction proceeds via butyl-d_1 intermediates in more than 90%. This result is contradictory to Horiuti–Polanyi mechanism, because the intermediates for the hydrogenation reaction are distinctive from those of the isomerization reaction. This fact indicates that the two reactions independently proceed on the different sites on the MoS_2 surface [17–22]. It is evident that the active sites for the isomerization reaction have no ability to hydrogenate the alkyl intermediates. If this is the case, it should be realized that we could not deduce the intermediates of the hydrogenation of olefins by investigating the isotopic hydrogen exchange of olefins because the isotopic exchange via alkyls is promoted on the sites for the isomerization reaction. Taking this fact into account, we can deduce the following important conclusion 'true intermediates can be deduced only from the products by reading the memory about the intermediates'. This means that the true intermediates for the hydrogenation reaction of olefins can be deduced only when we can decipher the information of intermediates memorized in the alkanes. Based on this conclusion, we developed a new method by which we can deduce the reaction intermediates of the hydrogenation reaction, which is the orientation in the addition of HD molecule to olefins [18–20]. When the molecularity of H_2, D_2, and HD is retained in the products of the hydrogenation reaction of olefins, the feature of alkyl intermediates will be reflected by the orientation in the addition of HD molecule, where the isotope effect is allowed by comparing the addition of H_2 and D_2 to olefins. The intermediates for the hydrogenation of propene, but-1-ene, but-1,4-diene, methyl acetylene and allene were deduced by using this method [14,17]. In case of MoS_2 surface, when MoS_2 is exposed to H_2, mono-hydride ($-MoH$) and di-hydride ($-MoH_2$) sites are formed on the edge surface of the lamella crystal. Mono-hydride sites ($-MoH$) can catalyze the isomerization reaction of olefins but have no ability to promote the hydrogenation of olefins. The catalytic hydrogenation reaction actually takes place on the di-hydride ($-MoH_2$) sites. As the reverse process of the formation of aklyl intermediates on the di-hydride sites is rather slow so that the di-hydride sites contribute little to the isomerization reaction. As a result, these two reactions via alkyl intermediates are described by the two catalytic cycles working independently as described by Scheme 1.

Another interesting example of the formation of active sites or compounds was found on a carbon doped with potassium carbonate. When a potassium carbonate doped carbon was evacuated at 650 C, the amount of potassium is markedly decreased from the surface although the temperature is lower than the decomposition temperature of potassium carbonate. This evacuated carbon surface was entirely inactive for the isomerization of but-1-ene [23]. When a small amount of O_2 is added to but-1-ene, however, but-1-ene was selectively isomerized to *cis*-but-2-ene as shown in Fig. 1. Coisomerization of but-1-ene and perdeutero but-1-ene proved that the isomerization reaction is brought about by intra-molecular hydrogen transfer mechanism [24,25].

In this case, potassium atoms dissolved in carbon undergo segregation by reacting with O_2 and specific active sites or compound are formed on the surface, and an intra-molecular hydrogen transfer reaction of *n*-butenes is promoted on this newly formed compound. More recently, Boffa et al. [26]

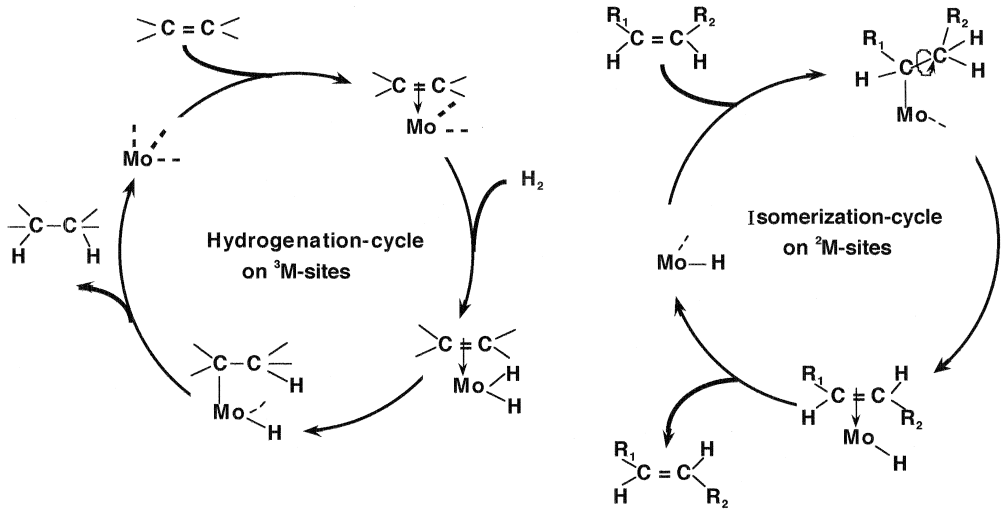

Scheme 1. Catalytic isomerization of olefins on mono-hydride (–MoH) sites and catalytic hydrogenation of olefins on dihydride ($-MoH_2$) sites formed on the edge surface of MoS_2 by exposing to H_2.

showed the formation of specific sites on Rh when a 0.5 monolayer of various oxides is grown on it, where the hydrogenation of CO, CO_2 and acetone is catalyzed. An interesting fact is that the catalytic activity of these newly formed active sites has a good correlation to the electronegativity of metal ions (X_i) of the oxides formed on Rh, where X_i is Tanaka's electronegativity of metal ion given by an equation of $X_i = (1 + 2Z)X_o$ [27], where Z is the valence of metal ion and X_o is the electronegativity of metal atom. The active sites are speculated to be formed at the boundary of the oxide islands on Rh but the real structure are not defined.

From these phenomena, we could say that the active sites or the functional compounds being responsible for the catalysis are so often synthesized by the reaction of substrate atoms with adsorbed molecules. According to the idea of synthesis of active sites, we can design highly selective and highly active catalysts. A good example is the preparation of super active olefin metathesis catalyst.

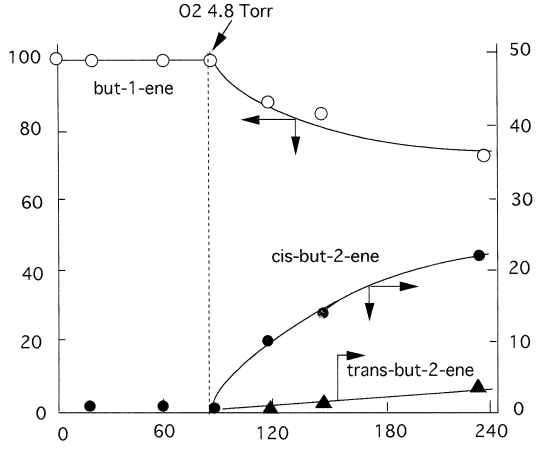

Fig. 1. Isomerization reaction of but-1-ene to but-2-ene by intramolecular hydrogen transfer mechanism is promoted by adding O_2 on a K_2CO_3 doped carbon.

We can provide highly selective super active olefin metathesis catalyst by preparing tailored active sites on MoO_x and/or WO_x surfaces. For example, MoO_x film sublimated on glass or quartz wall is entirely inactive, on which neither the metathesis reaction nor the isomerization reaction of olefins occur. That is, neither Mo = CH–R sites nor (–Mo–H) sites are formed by simple adsorption of olefins or H_2 on the MoO_x film. However, when Mo = CH–R sites were provided on this inactive MoO_x film by a chemical reaction, the inactive MoO_x film changed to a highly active and highly selective olefin metathesis catalyst as shown in Fig. 2. It is note worthy fact that this tailored surface has super activity for the olefin metathesis reaction but has no catalytic activity for the isomerization of olefins [28–30].

It is known that propene undergoes the following two types of metathesis reactions, one is the productive metathesis [i] and the other is degenerate or cross metathesis [ii].

$$CH_2{=}CH{-}CH_3 + CD_2{=}CD{-}CD_3 \begin{cases} \rightarrow CH_2{=}CD_2 + CD_3{-}CD{=}CH{-}CH_3 & \text{[i]} \\ \rightarrow CD_2{=}CH{-}CH_3 + CH_2{=}CD{-}CD_3 & \text{[ii]} \end{cases} \quad (2)$$

As Mo = CH–R sites can promote the olefin metathesis reaction but not the isomerization and/or the hydrogen scrambling reactions. Therefore, we used deuterium labeled olefins to investigate the

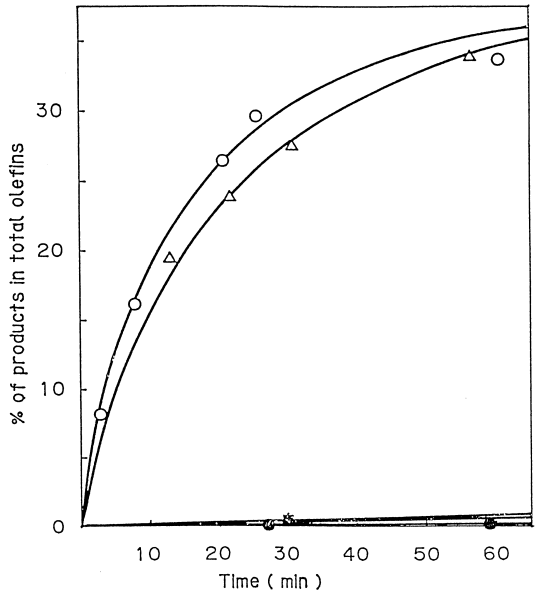

Fig. 2. Propene metathesis reaction at room temperature on functionalized MoO_x films, where the film is functionalized by reacting condensed propene (○) and ethylene (△) with H atoms at liquid nitrogen temperature, as prepared MoO_x film (●), reduced MoO_x film (▲), and MoO_x film treated with H-atom (■).

olefin metathesis reaction, and a total mechanism for the metathesis reaction of propene has been established by performing the following four deuterium labeled experiments [31]:

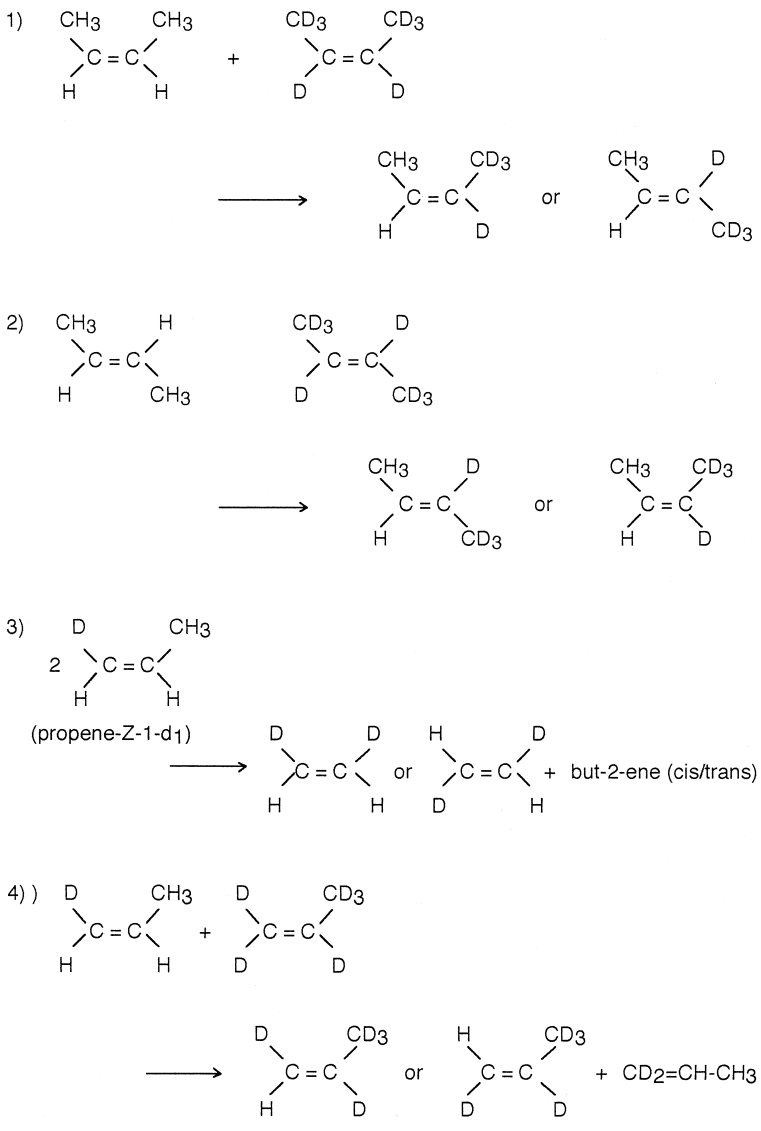

A total mechanism for propene metathesis reaction shown in Scheme 2 has been deduced from the conformation of metalla-cyclobutane intermediates by a series of labeled experiments [31]. That is, the conformational memory of the metalla-cyclobutane intermediates derived is deciphered by analyzing the labeled products, where we found that the conformation of parent olefins is transmitted to the daughter olefins when the metallacyclobutane intermediates involves more than two alkyl substitutes because stereo-structure of the metalla-cyclobutane can be retained by the two or more alkyl substituents. On the basis of conformational memory in the products, we succeeded in

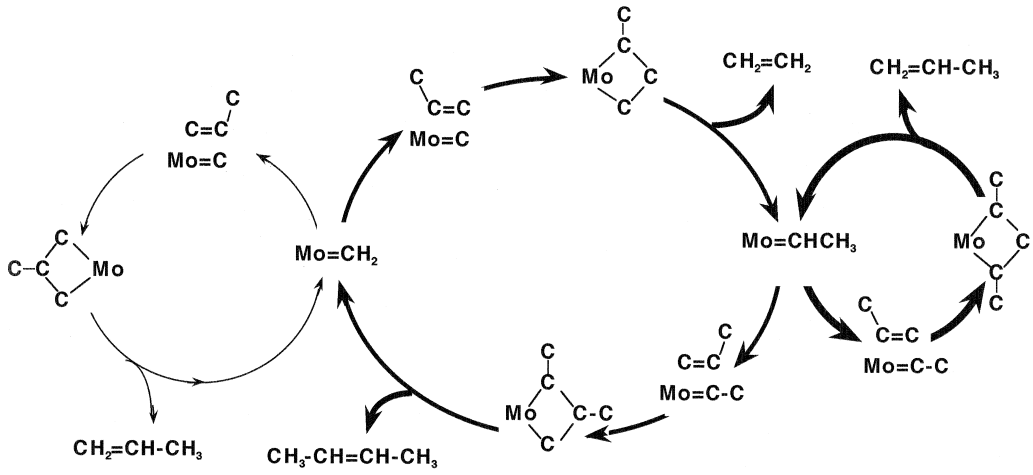

Scheme 2. Total mechanism for the metathesis reaction of propene. Middle cycle is responsible for the productive metathesis and the other two cycles are the cycles for the degenerate metathesis of propene but one degenerate metathesis cycle contributes little to the reaction.

deciphering the structural memory of the metalla-cyclobutanes intermediates and deciding the reaction route.

In Scheme 2, it is known that the productive metathesis of propene is brought about by alternative formation of $Mo=CH_2$ and $Mo=CH{-}CH_3$ intermediates. On the other hand, the degenerate metathesis reaction is promoted by a catalytic cycle via either $Mo=CH_2$ or $Mo=CH{-}CH_3$ intermediates. Therefore, it should be an interesting question that either $Mo=CH_2$ or $Mo=CH{-}CH_3$ predominantly contributes to the degenerate metathesis of propene. A labeled experiments using propene-*Z*-1-d_1 and propene-d_6 (reaction 4) proved that the degenerate metathesis of propene predominantly occurs via $Mo=CH{-}CH_3$ intermediates, because the *Z*-1-d_1 conformation is retained in the daughter propene molecules produced by the degenerate metathesis, that is, the degenerate metathesis of propene proceeds via the metallacyclobutane intermediates with two alkyl substituents which is not the catalytic cycle via the $Mo=CH_2$ but the cycle via the $Mo=CH{-}CH_3$ intermediates.

Why the degenerate metathesis reaction proceeds via $Mo=CH{-}CH_3$ intermediates instead of $Mo=CH_2$. It is well rationalized by the different reactivity depending on the orientation of propene molecules to $Mo=CH_2$ and $Mo=CH{-}CH_3$ intermediates as described below. This different reactivity of propene depending on the orientation to the $Mo=CH_2$ and $Mo=CH{-}CH_3$ intermediates as described below can explain also why the degenerate metathesis reaction [ii] is several ten times faster than the productive metathesis reaction [i].

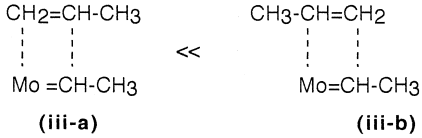

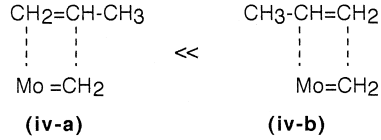

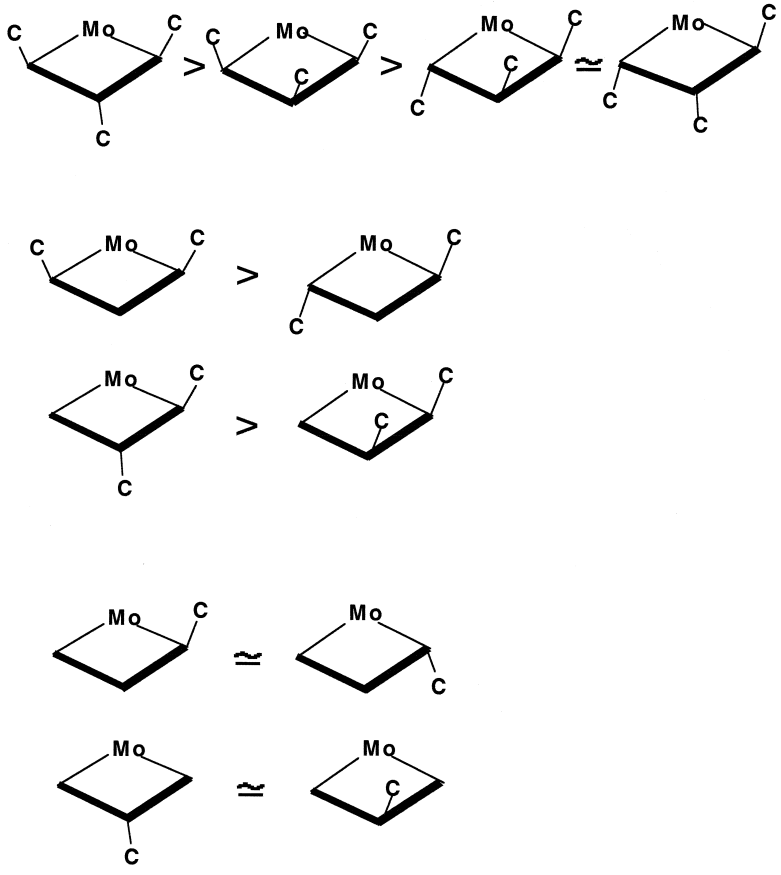

Scheme 3. Kinetically decided preferable conformational series of tri-substituted, di-substituted, and mono-substituted metallacyclobutane intermediates.

Taking account of the fact that because the reaction (iv-b) is several ten times faster than (iv-a), $Mo=CH-CH_3$ intermediates are predominant species on the active sites during propene metathesis reaction. From the conformation retaining selectivity determined by the metathesis of the labeled olefins, we can derive such a conformational sequence of the metalla-cyclobutanes as shown in Scheme 3, which is a kinetically deduced sequence of the alkyl substituted metallacyclobutane. It should be pointed out that the metallacyclobutane is not a flat ring but is bent. Therefore, the stereochemical conformation of the intermediates should be more complex but it is hard to deduce such stereochemical conformation by such a kinetic method shown here.

3. Catalytic reactions on well defined metal surfaces

More direct evidences for the formation of active sites or active compounds are expected on well defined single crystal surfaces. For this viewpoint, it is an interesting phenomenon that some catalytic reactions are structure sensitive but the others are not structure insensitive. As it was mentioned

above, any catalytic reaction is composed of several elementary processes and the structure sensitivity should be explained in relation to the rate determining step [14,17].

As Goodman et al. [32,33] showed, the methanation reaction on nickel catalyst, $CO + 3H_2 \rightarrow CH_4 + H_2O$, is a typical structure insensitive reaction. They also showed that the carbidic carbon formed on Ni surface is the key intermediates for methane formation reaction and the steady state concentration of carbidic carbon intermediates is given by a dynamic balance of the formation and the hydrogenation of carbidic carbon.

On the other hand, it is well known that the segregation of carbon on Ni(100), Ni(110), and Ni(111) surfaces undergoes reconstruction of the surfaces forming p4g(2×2) Ni(100)–C, p(4×5) Ni(110)–C, and complex $\begin{pmatrix} 7 & 2 \\ 4 & 7 \end{pmatrix}$ Ni(111)–C structures. The carbidic carbon formed on these Ni surfaces undergoes decomposition at the same temperature as shown in Fig. 3 although their ordered structures are different [34]. These facts suggest that a common carbidic carbon are formed on these Ni surfaces, which may be responsible for the structure insensitive catalytic activity of these Ni surfaces for the methane formation reaction. The reaction of carbidic carbon on a Ni(100) surface with H_2 showed the formation of CH species by the HREELS [35,36]. A common carbidic carbon formed on the Ni surfaces may be described by a formula of Ni_4C, and the reconstruction is brought about by ordered array of Ni_4C differently on the different crystallographic planes. Klink et al. [37] studied the formation of carbidic carbon on the three Ni single crystal surfaces by the STM. They showed that when a carbon atom is segregated on a Ni(100) surface and a Ni_4C is produced on the surface, the four Ni atoms displaces away a short distance from their original position, which induces strain on the surface. When the amount of carbidic carbon will exceed ca. 0.2 monolayer, a rotational relaxation occurs to remove the stress and a p(2×2)p4g Ni(100)–C structure is established. When a

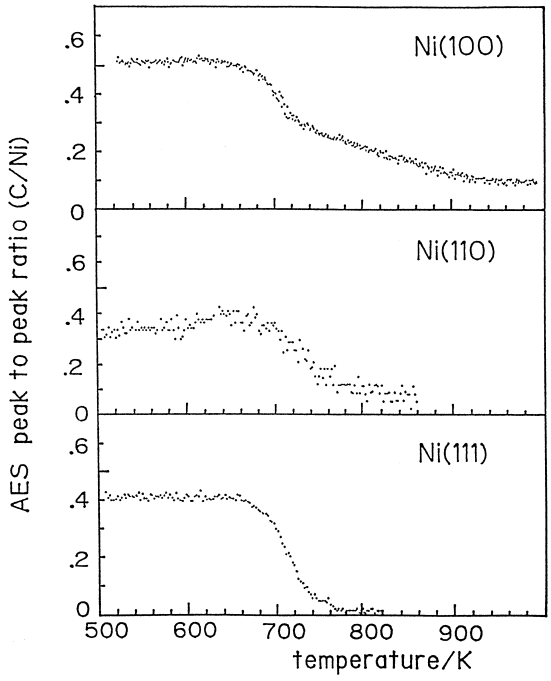

Fig. 3. Decomposition of surface carbide on Ni(100), Ni(110), and Ni(111) surfaces by raising temperature.

p(2 × 2)p4g Ni(100)–C surface is exposed to H atoms, the stress is markedly reduced by forming CH species and the p(2 × 2)p4g structure is relaxed to the p(2 × 2) structure [38]. These phenomena seem to support an idea of the formation of Ni_4C and their characteristic ordering on the three Ni surfaces.

As it was mentioned above, ammonia synthesis reaction on Fe single crystal obeys to an activity sequence of Fe(111) ≫ Fe(100) > Fe(110). Somorjai et al. [6,7] found an interesting phenomenon that when the alumina deposited Fe surfaces are activated by heating in $N_2 + H_2$ or in NH_3, the Fe(100) and Fe(110) surfaces are dramatically activated and their catalytic activity are almost equal to that of Fe(111) surface. So far the role of alumina in an industrial doubly promoted ammonia synthesis catalyst has been empirically explained as a stabilizer against the sintering of the surface, but the result proves entirely different role of alumina. That is, a surface compound of $FeAl_2O_4$ over-layer is formed by the reaction of alumina with Fe atoms on the Fe(100) and Fe(110), and a Fe(111) like layer

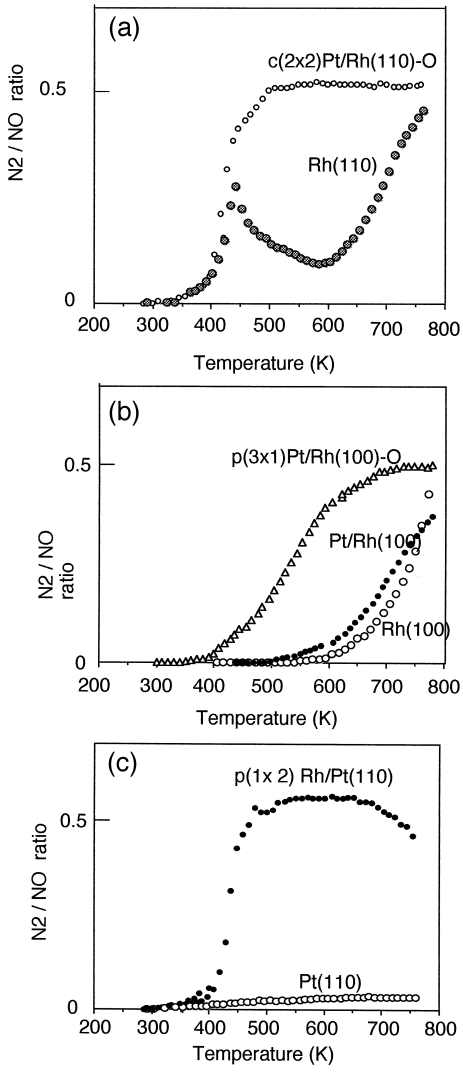

Fig. 4. Catalytic activity of Pt(100), Pt(110), Rh(100) surfaces and their bimetallic surfaces for the reaction of $NO + H_2$. (a) TPR in a flow of a mixture of $NO + H_2$ on Rh(110), c(2×2)Pt/Rh(100)-surfaces. (b) TPR in a flow of a mixture of $NO + H_2$ on Rh(100), as deposited Pt/Rh(100) and p(3×1)Rh/Pt(100)–O surfaces.

is grown over the $FeAl_2O_4$ layer so that the catalytic activity of these surfaces becomes almost equal to that of Fe(111) surface [6,7].

Another interesting activation of the surface has been observed on Pt–Rh catalyst by Tanaka et al. [8–11,39–44]. In this case, a specific active structure formed by reacting Rh atoms with oxygen may be responsible for the prominent catalytic activity of Pt–Rh bimetallic catalyst for removing NO_x, CO, and hydrocarbons in the automotive exhaust gas. That is, when a Pt–Rh(100) alloy surface is exposed to O_2 or NO, the surface undergoes a dramatical reconstruction accompanying the segregation of Rh with increasing adsorbed oxygen at around 500 K [9,10].

The Pt–Rh(100) alloy surface hard to take an equilibrium composition by annealing in vacuum at temperature lower than 900 K. It is quite different in O_2 and/or NO, that is, Rh atoms are readily segregated even at 450 K and undergoes the surface reconstruction, so we named it 'chemical reconstruction'. An interesting fact is that this reconstruction corresponds to the activation of Pt–Rh catalyst [39–42]. In order to shed light on the mechanism of the activation of Pt–Rh catalyst, we have studied a series of bimetallic model surfaces, which are Rh/Pt(100), Rh/Pt(110), Pt/Rh(100), and Pt/Rh(110) prepared by electrochemical deposition of Rh or Pt atoms onto the corresponding single crystal metal surfaces in a UHV-Electro-chemical chamber [43].

As shown in Fig. 4(a)–(c), catalytic reaction of $NO + H_2 \rightarrow 1/2N_2 + H_2O$ is highly structure sensitive on Pt and Rh surfaces and their catalytic activity is in a sequence of Pt(100) ≫ Pt(110) and

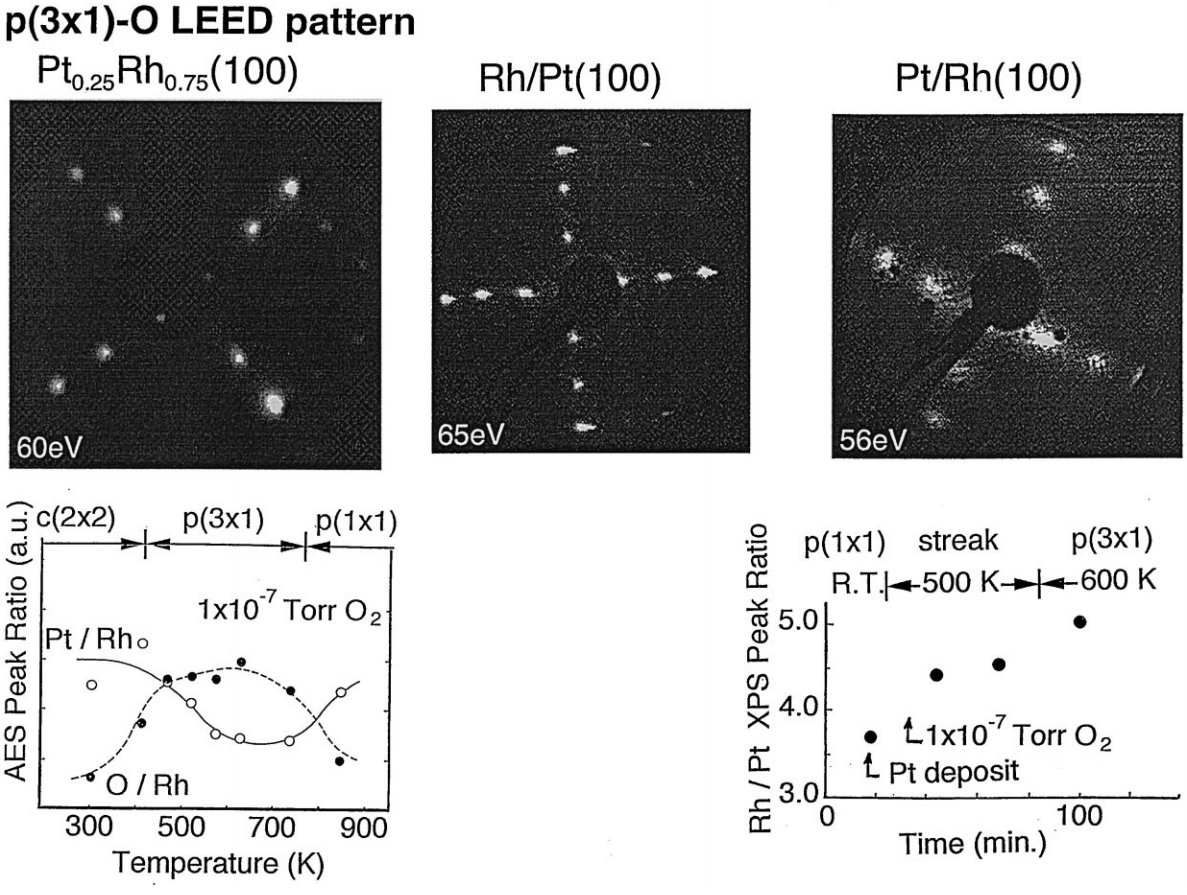

Fig. 5. A common p(3 × 1) LEED pattern observed on Pt/Rh(100), Rh/Pt(100), and Pt–Rh(100) alloy surfaces by heating in O_2.

Rh(110) > Rh(100). It is worthy of note that Pt(110) surface is almost inactive for this reaction and Rh(100) surface is also poorly active at temperature lower than 650 K. However, Rh deposited Pt(110) as well as Pt deposited Rh(100) bimetallic surfaces are markedly activated by heating in O_2 or NO, where the surfaces undergo reconstruction forming a c(2 × 2) Rh/Pt(110)–O and p(3 × 1) Pt/Rh(100)–O structures. An interesting fact is that as deposited Pt/Rh(100) surface is not so active as shown in Fig. 4(b), but the activity is markedly enhanced by the reconstruction forming the p(3 × 1) structure and its activity is almost equal to that of c(2 × 2) Rh/Pt(110)–O and p(3 × 1) Pt–Rh(100)–O alloy surfaces. It was confirmed that when a Pt deposited Rh(110) surface is heated in O_2, the surface undergoes reconstruction forming a c(2 × 4)Pt/Rh(110) structure, and the catalytic activity is markedly enhanced. The activated bimetallic surfaces of c(2 × 2)Rh/Pt(110)–O, p(3 × 1)Pt/Rh(100)–O, p(3 × 1)Rh/Pt(100)–O, and c(2 × 4)Pt/Rh(110)–O as well as the activated p(3 × 1)$Pt_{0.25}Rh_{0.75}$(100)–O alloy surface have almost equal catalytic activity for the reaction of $NO + H_2$ 1/2 $N_2 + H_2O$ as shown in Fig. 4. From these results, we can conclude that the Pt–Rh bimetallic and/or alloy surfaces are activated by forming active sites with a common local structure on the surfaces, which reflects the same catalytic activity of these surfaces. As it was cited above, Pt–Rh alloy surfaces undergo chemical reconstruction with the segregation of Rh at ca. 450 K when the surface is heated in O_2 or NO, and the p(3 × 1) LEED pattern is commonly established on the Pt/Rh(100), Rh/Pt(100), and $Pt_{0.25}Rh_{0.75}$(100) alloy surfaces as shown in Fig. 5 [12,44]. An STM image for a p(3 × 1)$Pt_{0.25}Rh_{0.75}$(100)–O surface is shown in Fig. 6 [13].

As it was mentioned above, the catalytic activity of the reconstructed Rh/Pt(110) and Pt/Rh(110) surfaces is almost equal to that of the p(3 × 1)Rh/Pt(100)–O, p(3 × 1)Pt/Rh(100)–O, and the p(3 × 1)$Pt_{0.25}Rh_{0.75}$(100)–O surfaces. The Rh/Pt(110) surface annealed in O_2 gives a c(2 × 2) LEED pattern and is readily changed to a p(1 × 2) LEED pattern at room temperature by exposing to hydrogen. On the other hand, the Pt/Rh(110) surface annealed in O_2 gives a c(2 × 4) LEED pattern. If these reconstructed surfaces are composed of active sites with a common local structure, we can

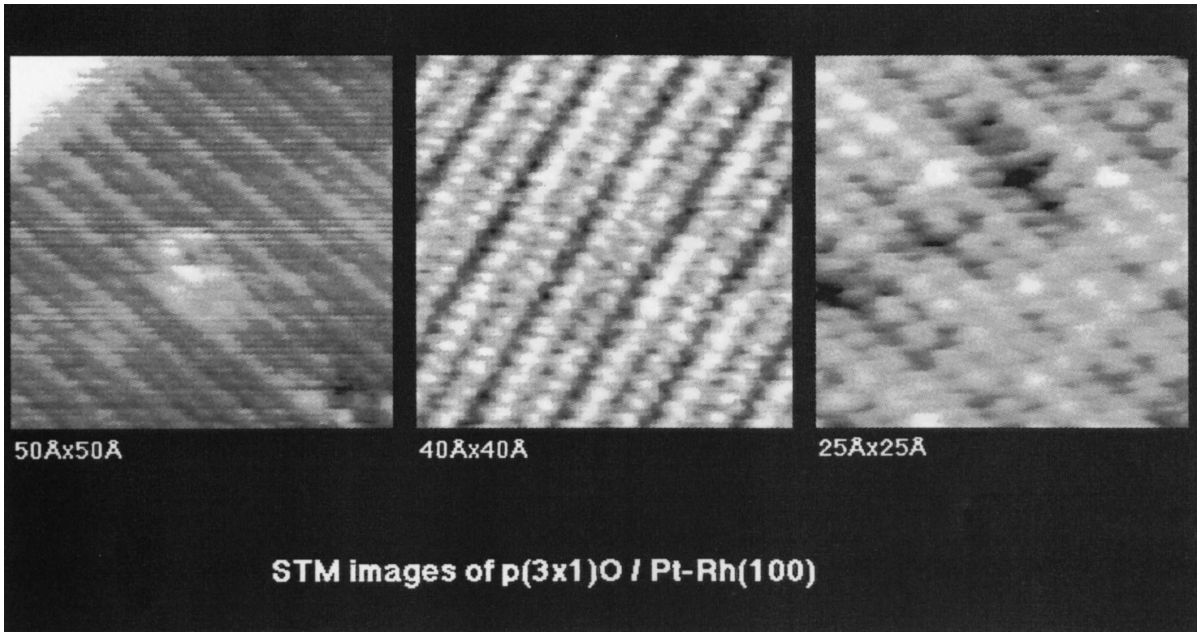

Fig. 6. STM image for a p(3 × 1) $Pt_{0.25}Rh_{0.75}$(100)–O surface, which gave the three different images depending on the tip condition. One STM image reflects the whole metal atoms in almost equal intensity but the other two images correspond to either of Pt or Rh atoms.

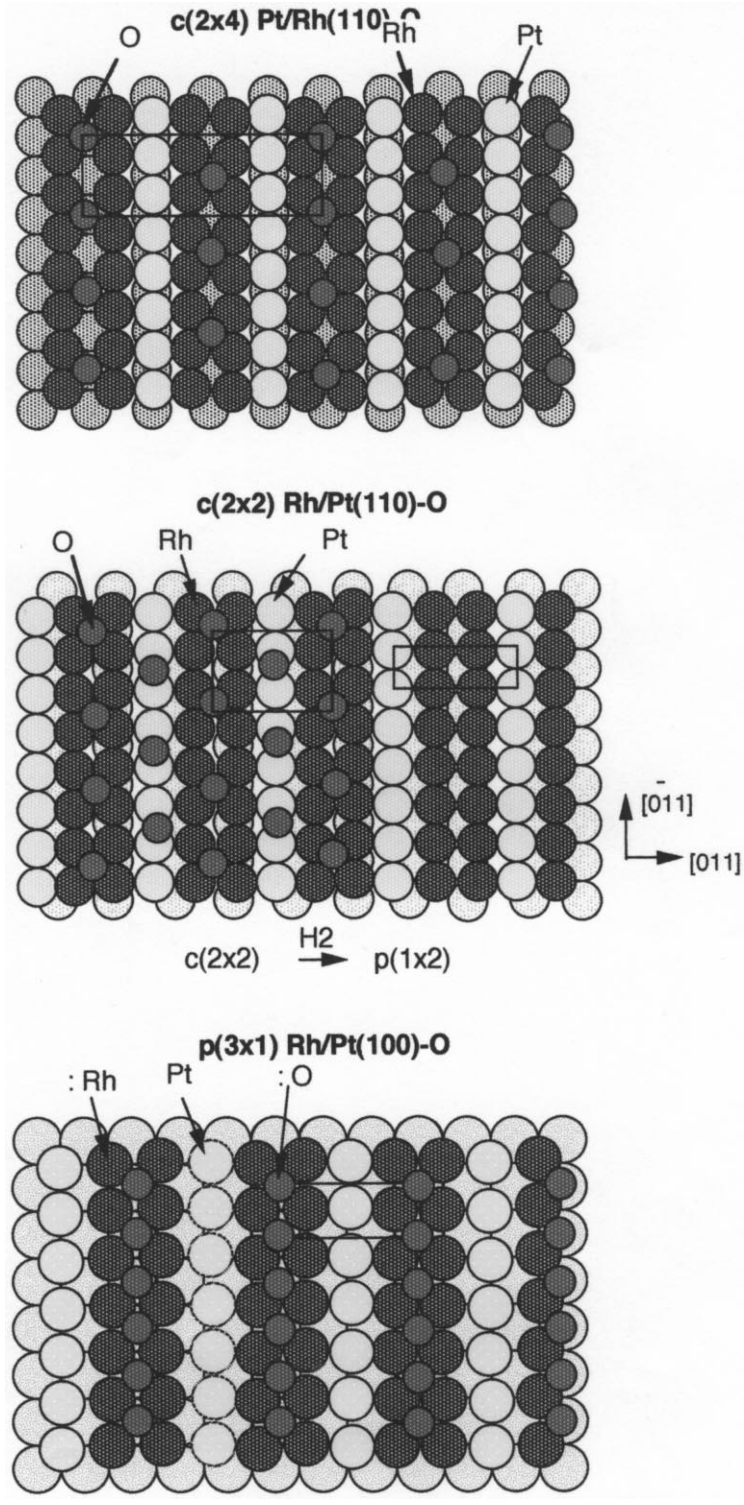

Fig. 7. Models for the $p(3\times1)Rh/Pt(100)-O$, $c(2\times4)Pt/Rh(110)-O$, and $c(2\times2)$ $Rh/Pt(110)-O$ surfaces deduced from the $p(3\times1)Pt_{0.25}Rh_{0.75}(100)-O$ surface.

speculate the p(3 × 1)Rh/Pt(100)–O, c(2 × 4)Pt/Rh(110)–O, and c(2 × 2) Rh/Pt(110)–O surfaces in relation to the p(3 × 1) $Pt_{0.25}Rh_{0.75}$(100)–O surface deduced by the STM as shown in Fig. 7.

From these empirical relations between the catalytic activity and the surface structure, we could derive a general conclusion that 'a well developed catalyst (optimized catalyst) will be structure insensitive because they could provide the highest density of active sites'. This will be a guiding principle for designing perfectly improved catalyst.

4. Bifunctional processes on Cu/Pd(111) surfaces

In-situ measurement of the catalyst surface has acquired additional importance of the spatial resolution of order of angstrom and time resolution of a few tenth of seconds, which allows us to detect the dynamic behaviour of the individual atoms. At this point, the origin of inhomogenous reactivity of the metal atoms and the adsorbed species influenced by local electronic states, local structure and specific chemical construction of the active sites, and the diffusion of the reactive species between the different active sites has been proved by the STM in atom scale.

As it was discussed above, the activation of catalyst is regarded by the creation or modification of reactive surface during catalysis. Such surface activation closely relates to the modification of geometric and electronic structure of active sites. Especially the modification of bifunctional or multifunctional surfaces is interesting because reactive intermediate species may diffuse between the different active sites.

The improvement of STM experimental techniques allowed us to understand the atom-by-atom alloying process on the bimetallic surfaces [45–47], and the diffusion of atoms and/or molecules on the surface is now directly proved by the STM [48]. This development now enable us to throw a light on chemical properties of bifunctional catalysts, e.g., bimetallic surfaces, to atomic-scale phenomena, and the mechanisms of the activation on an atomic scale.

The reaction of O_2 and H_2 on Cu/Pd(111) bimetallic surfaces provides a model defined on an atomic scale. Using STM and XPS complementary, we revealed the structural modification of active species and the spatial distribution of active sites in relation to the chemical reactivity of the surface.

As shown in Fig. 8a, our STM image proves that submonolayer Cu evaporated onto a Pd(111) surface grows in a single atom layer at RT, as LEED I–V study reported [49]. It is noted that the straight troughs running parallel to step edges divide the traces into two differently imaged regions. The regions from the straight troughs down to lower step edges increased with increasing evaporated Cu atoms, indicating these regions contain Cu atoms. The regions from the straight lines up to upper step edges are imaged with the same periodicity of a clean Pd(111) surface. This arrangement shows the growth of a single Cu atom layer by step flow mode in submonolayer range. The regions from the straight troughs down to lower step edges are imaged in atomic resolution in Fig. 8b. It is noted that monoatomic protrusions were imaged brightly on the atop site of monolayer Cu islands. After annealing these surfaces to 470 K in UHV, number of these protrusions increased in Cu regions, and mono atomic dark dents appeared on the atop site of Pd substrate near to step edges of Cu islands. Based upon these fact, we deduced that the bright mono atomic protrusions in Cu regions correspond to Pd atoms alloyed into Cu islands by atom replacement. The dark mono atomic dents on the Pd substrate were assigned to Cu atoms alloy into the Pd substrate. STM studies of a Pd/Cu(100) surface reported similar contrast of the elements [50,51].

When a Cu/Pd(111) surface is exposed to O_2 at RT, bright triangular features and dark hexagonal features are increased as shown in Fig. 9, with concomitant decline of the step edges of Cu islands.

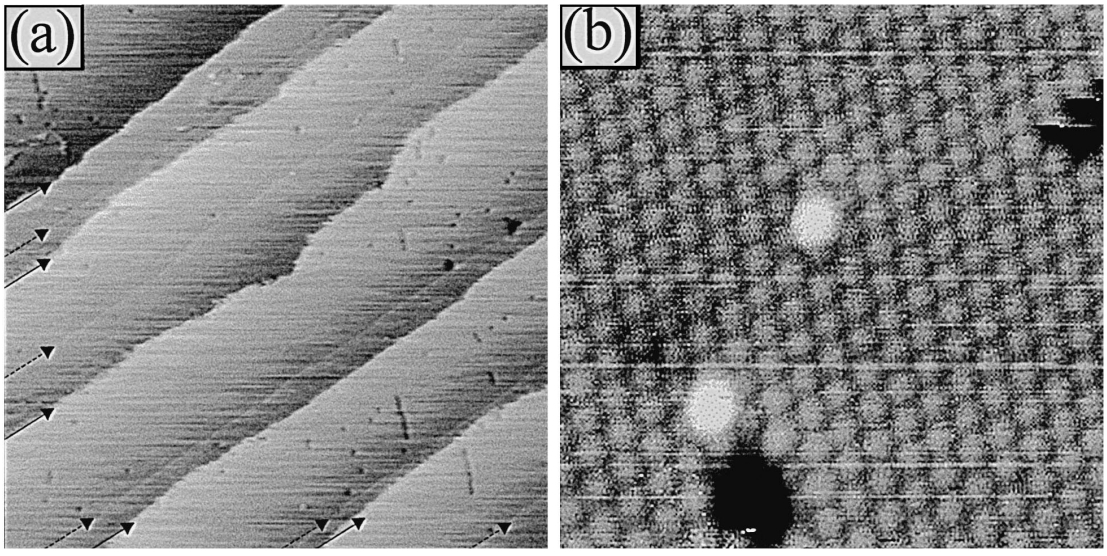

Fig. 8. Two STM images of submonolayer Cu evaporated onto a Pd(111) surface at RT. (a) A 586×616 Å^2 STM image. Submonolayer Cu grew as a single layer in step flow mode. Troughs pointed by drawn dashed arrows are original Pd step edges, and solid arrows point step edges. (b) A 41×43 Å^2 STM image of Cu region with atomic resolution. Bright mono atomic protrusions correspond to Pd atoms alloyed into a Cu layer.

Evaporation of Cu atoms in the presence of ambient O_2 forms the dark hexagonal features only. In comparison the STM image to the XPS spectrum of the Cu/Pd(111) surface, a kinetic energy of Cu L_3VV Auger peak made shift by exposing to oxygen, but no chemical shift in binding energy of Cu $2p_{2/3}$ state nor appearance of Cu $2p_{2/3}$ satellite were detected. These facts indicate the formation of Cu_2O like species on the surface in the presence of O_2.

On the other hand, SEXAFS study reported that exposure of a Cu(111) surface to O_2 leads to the formation of Cu_2O species at RT [52]. Combining with the ion scattering experiment and the STM, Jensen et al. [53,54] showed that O_2 exposure at higher temperature leads to the formation of Cu_2O(111) layers on a Cu(111) surface, and the STM image gives a quasi hexagonal feature.

Reduction of the dark hexagonal features formed on the Pd(111) surface, as described below, yielded a 0.7 ML equivalent Cu atoms release, which correspond to the same number of Cu atoms in a monolayer of bulk Cu_2O(111). The decline of step edges of Cu islands with the formation of the dark hexagonal and bright triangular features indicates that the bright triangular features contain more than 1 ML of Cu. Based upon these results, we assigned the dark hexagonal features to Cu_2O species formed on a Pd(111) surface and the bright triangular features to Cu_2O grown on monolayer thick Cu islands.

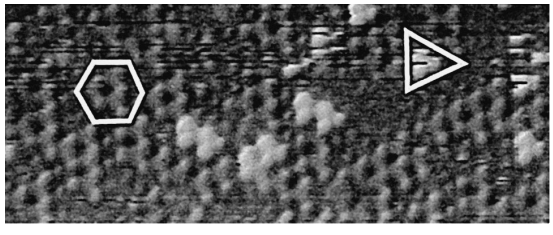

Fig. 9. A 166×88 Å^2 STM image of Cu region on a Cu/Pd(111) surface exposed to O_2 at RT. Bright triangular features and dark hexagonal features were imaged.

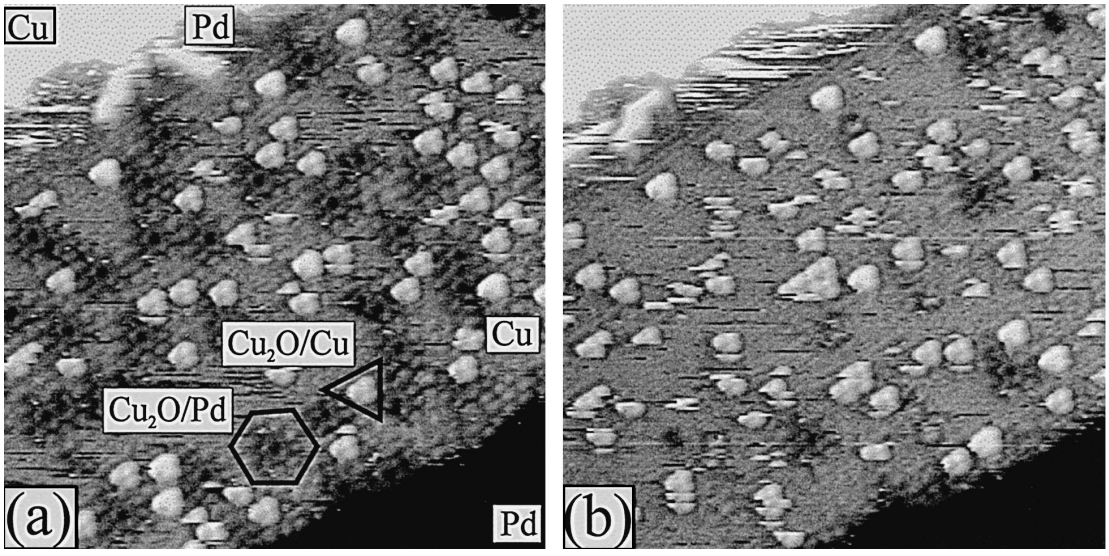

Fig. 10. Two 166×176 Å^2 sequential STM images of monolayer thick Cu islands on a Pd(111) surface under reaction of H_2 and O_2. (a) The surface was exposed to O_2 and H_2 in O_2 excess condition. From (a) to (b) the surface was exposed to H_2. Brightly imaged triangular features corresponds Cu_2O species on the Cu islands. Dark hexagonal Cu_2O species on the Pd substrate reacted with hydrogen even inside of Cu islands.

These two kinds of Cu_2O species show clear contrast in chemical reactivity, that is, Cu_2O species on the Pd(111) terrace react with H_2 at RT, but the Cu_2O species formed on the Cu layer can react with H_2 only above 350 K. Therefore, when the Pd(111) surface with both Cu_2O species is exposed to H_2 at RT, the Cu_2O species on a Pd(111) surface is preferentially decreased as shown in Fig. 10. Reduction of Cu_2O species on Pd with hydrogen starts all over the Cu islands when the coverage of Cu and the Cu_2O species is low. In contrast, when the coverage of Cu and the Cu_2O species is high, the reaction proceeds rather slowly at the virgin area of the Pd surface. Mass spectrometric analysis showed the formation of H_2O from the reaction and XPS spectrum shows the reversal chemical shifts of the Cu L_3VV Auger after this reduction.

As it is well known that dissociative adsorption of H_2 rapidly undergoes on Pd(111), but is very slow on Cu(111) and Cu thin layer [55,56]. The catalytic reaction between O_2 and H_2 proceeds rapidly even at low temperature on Pd(111) surface, but its rate is negligible on Cu(111) surface [57]. The reaction of the Cu_2O species with H_2 depends upon area of uncovered Pd atoms and upon local distance to the area indicates the presence of diffusion of atomic hydrogen from Pd areas to Cu islands.

In conclusion, the reactivity of the $Cu_2O/Pd(111)$ species depends upon local arrangement of the sites for H_2 dissociation. We demonstrated here that the in-situ measurements of catalytic reactions, on an atomic scale, enabled us to directly correlate physical processes such as structural modification of intermediates and rearrangement of active sites inducing diffusion of reactive species between different active sites, to the activation process of catalyst.

References

[1] J. Horiuti, Adv. Catalysis IX (1957) 339.
[2] K. Tamaru, Adv. Catalysis 15 (1964) 65.

[3] K. Tamaru, Dynamic Heterogeneous Catalysis, Academy Press, London, 1978.
[4] M. Boudart, A. Aldag, J.E. Benson, N.A. Dougerty, C.G. Harkins, J. Catal. 6 (1966) 92.
[5] S.L. Bernasek, W.J. Siekhause, G.A. Somorjai, Phys. Rev. Lett. 30 (1973) 1202.
[6] S.R. Bare, D.R. Strongin, G.A. Somorjai, J. Phys. Chem. 90 (1986) 4726.
[7] D.R. Strongin, S.R. Bare, G.A. Somorjai, J. Catal. 103 (1987) 289.
[8] A. Sasahara, H. Tamura, K. Tanaka, J. Phys. Chem. 100 (1996) 15229.
[9] H. Hirano, T. Yamada, K. Tanaka, J. Siera, B.E. Nieuwenhuys, Vacuum 41 (1990) 134.
[10] H. Hirano, T. Yamada, K. Tanaka, J. Siera, B.E. Nieuwnhuys, Surf. Sci. 222 (1989) L804.
[11] T. Yamada, H. Hirano, J. Siera, B.E. Nieuwenhuys, K. Tanaka, Surf. Sci. 226 (1990) 1.
[12] H. Tamura, K. Tanaka, Langmuir 10 (1994) 4530.
[13] Y. Matsumoto, Y. Okawa, T. Fujita, K. Tanaka, Surf. Sci. 355 (1996) 109.
[14] K. Tanaka, Adv. Catalysis 33 (1985) 99.
[15] M. Polanyi, J. Horiuti, Trans. Farady Soc. 30 (1934) 1164.
[16] J. Horiuti, Proc. 2nd Intern. Cong. on Catal. (Paris) 1 (1961) 1191.
[17] K. Tanaka, T. Okuhara, Catal. Rev. Sci. Eng. 15 (1977) 249.
[18] K. Tanaka, T. Okuhara, S. Sato, K. Miyahara, J. Catal. 43 (1976) 360.
[19] T. Okuhara, K. Tanaka, JCS Faraday Trans., I 75 (1979) 245.
[20] K. Tanaka, T. Okuhara, J. Catal. 78 (1982) 155.
[21] T. Okuhara, K. Tanaka, JCS Faraday Trans., I 75 (1979) 245.
[22] T. Okuhara, K. Tanaka, J. Am. Chem. Soc. 98 (1976) 7884.
[23] S. Yokoyama, K. Tanaka, I. Toyoshima, K. Miyahara, K. Yoshida, J. Tashiro, Chem. Lett. 399 (1980) .
[24] S. Yokoyama, K. Tanaka, J. Seisho, JCS Chem. Comm. 1061 (1981) .
[25] S. Yokoyama, K. Tanaka, H. Haneda, JCS Chem. Comm. 820 (1982) .
[26] A. Boffa, C. Lin, A.T. Bell, G.A. Somorjai, J. Catal. 149 (1994) 149.
[27] K. Tanaka, A. Ozaki, J. Catal. 8 (1967) 1.
[28] M. Kazuta, K. Tanaka, JCS Chem. Comm. 616 (1987) .
[29] M. Kazuta, K. Tanaka, Catal. Lett. 1 (1988) 7.
[30] M. Kazuta, K. Tanaka, J. Catal. 123 (1990) 164.
[31] K. Tanaka, K. Tanaka, H. Takeo, C. Matsumura, J. Am. Chem. Soc. 109 (1987) 2422.
[32] D.W. Goodman, R.D. Kelley, T.E. Madey, J.T. Yates Jr., J. Catal. 63 (1980) 226.
[33] D.W. Goodman, J. Vac. Sci. Technol. 20 (1982) 522.
[34] H. Hirano, K. Tanaka, J. Catal. 133 (1992) 461.
[35] H. He, J. Nakamura, K. Tanaka, Surf. Sci. 283 (1993) 117.
[36] H. He, Y. Okawa, K. Tanaka, Surf. Sci. 376 (1997) 310.
[37] C. Klink, L. Olsen, F. Besenbacher, I. Stensgaard, E. Laegsgaard, Phys. Lett. 71 (1993) 4350.
[38] H. He, Y. Okawa, K. Tanaka, Surf. Sci. 376 (1997) 310.
[39] A. Sasahara, H. Tamura, K. Tanaka, Catal. Lett. 28 (1994) 161.
[40] H. Tamura, A. Sasahara, K. Tanaka, Catalysis and Automotive Pollution Controll—III, 229–236. Studies in Surface Science and Catalysis, Vol. 96, Elsevier, 1995.
[41] A. Sasahara, H. Tamura, K. Tanaka, J. Phys. Chem. 100 (1996) 15229.
[42] A. Sasahara, H. Tamura, K. Tanaka, J. Phys. Chem. B 101 (1997) 1186.
[43] M. Taniguchi, E.K. Kuzembaev, K. Tanaka, Surf. Sci. Lett. 290 (1993) L711.
[44] H. Hirano, T. Yamada, K. Tanaka, J. Siera, B.E. Nieuwenhuys, Vacuum 41 (1990) 134.
[45] Bardi, Rep. Prog. Phys. 57 (1994) 939.
[46] J. Wintterlin, R.J. Behm, in: H.J. Guntherodt, P. Wiesendanger, Scanning Tunneling Microscopy I, Springer Verlag, 1994, pp. 390 and 253.
[47] F. Besenbacher, L.P. Nielsen, P.T. Sprunger, in: D.A. King, D.P. Woodruff, The Chemical Physics of Solid Surface and Heterogeneous Catalysis, Chap. 10, Elsevier, in press.
[48] D.J. Coulman, J. Wintterlin, R.J. Behm, G. Ertl, Phys. Rev. Lett. 64 (1990) 1761.
[49] H. Li, D. Tian, F. Jona, P. Marcus, Solid State Commun. 77 (1991) 651.
[50] P.W. Murry, I. Stensgaard, E. Laesgaard, F. Besenbacher, Phys. Rev. B 52 (1995) R14404.
[51] P.W. Murry, I. Stensgaard, E. Laesgaard, F. Besenbacher, Surf. Sci. 365 (1996) 591.
[52] J. Haase, H.J. Kuhr, Surf. Sci. 203 (1988) L695.
[53] F. Jensen, F. Besenbacher, I. Stensgaard, Surf. Sci. 259 (1991) L774.
[54] F. Jensen, F. Besenbacher, I. Stensgaard, Surf. Sci. 269–270 (1992) 400.
[55] Paffett, C.T. Cambell, T.N. Taylor, S. Srinivasan, Surf. Sci. 154 (1985) 284.
[56] B. Hammer, M. Scheffler, K.W. Jacobsen, J.K. Norskov, Phys. Rev. Lett 73 (1994) 1400.
[57] O.P. van Preussen, M.M.M. Dings, O.L.J. Gijzeman, Surf. Sci. 179 (1987) 377.